Time-dependent local potential in a Tomonaga-Luttinger liquid

Naushad Ahmad Kamar and Thierry Giamarchi
DQMP, University of Geneva, 24 Quai Ernest-Ansermet, CH-1211 Geneva, Switzerland
(Received 3 June 2017; published 26 December 2017)

We study the energy deposition in a one-dimensional interacting quantum system with a pointlike potential modulated in amplitude. The pointlike potential at position $x = 0$ has a constant part and a small oscillation in time with a frequency ω. We use bosonization, renormalization group, and linear response theory to calculate the corresponding energy deposition. It exhibits a power law behavior as a function of the frequency that reflects the Tomonaga-Luttinger liquid (TLL) nature of the system. Depending on the interactions in the system, characterized by the TLL parameter K of the system, a crossover between weak and strong coupling for the backscattering due to the potential is possible. We compute the frequency scale ω_*, at which such crossover exists. We find that the energy deposition due to the backscattering shows different exponents for $K > 1$ and $K < 1$. We discuss possible experimental consequences, in the context of cold atomic gases, of our theoretical results.

DOI: 10.1103/PhysRevA.96.063620

I. INTRODUCTION

Cold atomic systems have proven in the recent year to be a remarkable playground to study the effect of strong correlations in quantum systems [1,2]. In particular they have allowed the realization of one-dimensional quantum systems both for bosons and for fermions. In one dimension, interactions between the particles lead to a very rich set of properties, very different from their higher dimensional counterparts. The general physics goes by the description known as Tomonaga-Luttinger liquid (TLL) [3–6].

In a TLL, the interactions lead to a critical state in which correlations decrease as power laws. This makes the system extremely sensitive to external perturbations, such as a periodic potential [7], quasiperiodic and disordered potentials [8,9], and even the presence of a single impurity [10,11]. In the later case depending on the interactions in the system even a single impurity can potentially completely block the system. Such effects have been investigated in the condensed matter context both in the context of carbon nanotubes [12] and also of edge states in the quantum Hall effect [13]. In such a context the main probe is connected to the transport through the impurity site, and the control parameters are either the temperature or the voltage. Theoretically, transport through a weak oscillating potential is studied and current through the oscillating potential shows a power law dependence on frequency [14–17].

In the present paper we propose to investigate the possibilities that are offered by the remarkable tunability and control of cold atom realization to study this class of effects. In particular we consider the question of a local potential, present in a one-dimensional system, that would be periodically modulated in time around an average value. Such a technique of periodically modulating potentials has been exploited with success to investigate several aspects of the Mott transition both in bosonic and fermionic systems [18,19], for disordered systems [20], or for superconducting systems [21]. A theoretical analysis shows that measuring quantities such as the deposited energy [22,23] or the rise of the number of doubly occupied sites [24,25], in response to a periodic global modulation provides a spectroscopic probe akin, but not alike the optical conductivity. We show here that the analysis of the deposited energy in the system as a function of the frequency dependence of the *local* modulation gives direct information on the physics of the static problem with the impurity [10,11]. The frequency dependence of the energy absorbed is a power law reflecting the TLL nature of the system.

The paper is structured as follows: In Sec. II, we introduce the model we use, within the framework of TLL to study the energy deposition by using linear response theory (LRT). Depending on the interaction two cases in which the impurity potential would be relevant (respectively, irrelevant) in the static case must be distinguished. Section III B discusses the deposited energy for the case in which the static impurity potential is irrelevant. This typically corresponds to $K > 1$ for the TLL. The opposite case of $K < 1$ is examined in Sec. III D. The results and their potential application to experimental systems in cold atomic gases are discussed in Sec. IV. The conclusion is given in Sec. V and some technical details are described in the appendixes.

II. MODEL AND METHOD

A. Model

We consider a one-dimensional system, schematically shown in Fig. 1. The system is made of interacting bosons or fermions described by a Hamiltonian H_0 which depends on the precise system under consideration (e.g., continuum or system on a lattice) and will be made more precise below. Most of this paper is concerned with a single component system, of bosons or fermions, but we also discuss briefly the case of a two-component fermionic system. This is particularly relevant in connection with recent realizations of the fermionic microscope [26,27] that allow the label of control relevant to carry the time of modulation and measurements corresponding to the present study. We consider separately the case of weak and strong potentials for a single-component case and then address the two-component weak potential case.

We add to this system a time-dependent potential $V(x,t)$. The total Hamiltonian we consider is, thus,

$$H = H_0 + H_{\rm imp},$$
$$H_{\rm imp} = \int dx\, V(x,t)\rho(x), \tag{1}$$

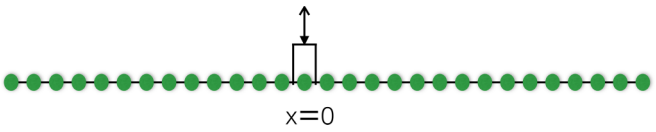

FIG. 1. Sketch of a one-dimensional system with a time-dependent external local potential $V(x=0,t) = V_0 + \delta V \cos(\omega t)$. The rectangular box represents a static potential V_0. The double head arrow represents the time-dependent part of the potential $\delta V \cos(\omega t)$.

where $\rho(x)$ represents the density of particles at position x. We compute here the change in energy caused by this *local* modulation. This corresponds to the local version of the shaking technique, in which a full optical lattice is modulated [22–24].

The modulation of the amplitude of the local potential is given by (see Fig. 1)

$$V(x,t) = [V_0 + \delta V \cos(\omega t)] f_\lambda(x), \tag{2}$$

where $f_\lambda(x)$ is a short-range function which is a regularized δ function. For simplicity we chose

$$f_\lambda(x) = \frac{1}{2\lambda \cosh^2(x/\lambda)}, \tag{3}$$

the δ function being reproduced in the limit $\lambda \to 0$.

Thus for (2) the impurity potential can be split in a purely static part corresponding to the one of a single impurity and a purely dynamical part, of mean zero. We can thus quite generally write

$$H = H_S + \cos(\omega t) O, \tag{4}$$

where H_S is the purely static impurity potential, and O the operator corresponding to the modulation given by (2).

If the impurity potential V_0 is weak compared to the kinetic and interaction energy of the system, then one has

$$H_S = H_0 + V_0 \int dx f_\lambda(x) \rho(x). \tag{5}$$

We consider that $f_\lambda(x)$ varies fast enough compared to the typical scales of the problem and thus can be assimilated to a $\delta(x)$ function as far as the density variation of the system is concerned.

Since the *perturbation* is small we use linear response theory. The energy deposition rate is given by (see Appendix A)

$$E_R = -\tfrac{1}{2}\omega \mathrm{Im}\chi^R(\omega), \tag{6}$$

where

$$\chi^R(\omega) = -i \int_0^\infty dt e^{i(\omega + i\delta)t} \langle [O(t), O(0)] \rangle \tag{7}$$

is the retarded correlation function of the operator O linked to the perturbation (see Appendix A). $\langle \cdots \rangle$ denotes the quantum and/or thermal average with the Hamiltonian H_S in (4).

B. Weak potential, bosonization

In order to treat the Hamiltonian (4) we use the bosonization technique. Indeed for one-dimensional quantum systems and regardless of the statistics of the particles, the low energy excitations of the system can be represented by the Hamiltonian [5]:

$$H_0 = \frac{1}{2\pi} \int dx \left[u K (\partial_x \theta(x))^2 + \frac{u}{K} (\partial_x \phi(x))^2 \right]. \tag{8}$$

The fields ϕ and θ are canonically conjugate,

$$\left[\phi(x), \frac{1}{\pi} \nabla \theta(x') \right] = i \delta(x - x'). \tag{9}$$

The field ϕ is related to the density of particles via

$$\rho(x) = \rho_0 - \frac{1}{\pi} \nabla \phi(x) + \rho_0 \sum_{p \neq 0} e^{i 2p(\pi \rho_0 x - \phi(x))}, \tag{10}$$

where ρ_0 is the average density of particles. Note that for fermions $2\pi\rho_0 = 2k_F$ where k_F is the Fermi wave vector. The above formula is the basis for the so-called bosonized representation, that relates the original Hamiltonian in terms of collective variables of density (ϕ) and current (θ). The transformation is by now standard and we refer the reader to the literature for more details [5].

In (8) u and K are known as Tomonaga-Luttinger liquid parameters and they depend in general on the properties of the system and in particular on the interactions between the particles. u is the velocity of sound excitations, while K is a dimensionless parameter controlling the decay of the correlation functions. For fermions, $K = 1$ for noninteracting particles while $K > 1$ (respectively, $K < 1$) for attraction (respectively, repulsion) between the particles. For bosons $K = \infty$ for noninteracting particles, and becomes smaller as the repulsion increases. For contact interaction only $K > 1$, with $K = 1$ being reached for infinite repulsion between the bosons (the so-called Tonks-Girardeau limit). Longer range interactions allow one in principle to reach any value of K. For special models such as the Lieb-Lininger model or the Bose-Hubbard one for bosons or the Hubbard model for fermions precise relations between the microscopic parameters and the TLL parameters are known [5,6]. In general if the microscopic parameters are known the TLL parameters can be computed with an arbitrary degree of accuracy. We thus use the Hamiltonians (8) and (4) with the representation (10) as our starting model in this paper.

The Hamiltonian H_S thus describes a TLL with a single impurity, for which physics is well known [10]. We briefly recall the main elements of this Hamiltonian since it will be needed to compute the effects of the dynamical perturbation.

For a perturbation weak compared to the kinetic and interaction energy, using (10) the impurity part becomes

$$\begin{aligned} H^0_{\mathrm{imp}} &= V_0 \int dx f_\lambda(x) \rho(x) \\ &= V_0 \int dx f_\lambda(x) \left[-\frac{1}{\pi} \nabla \phi(x) + 2\rho_0 \cos(2\phi(x)) \right], \end{aligned} \tag{11}$$

where we have kept only the lowest ($p = \pm 1$) and the most relevant harmonics in density (10).

The first term can be absorbed by a redefinition of the field ϕ,

$$\tilde{\phi}(x) = \phi(x) - \frac{K V_0}{u} \int_0^x dy f_\lambda(y). \tag{12}$$

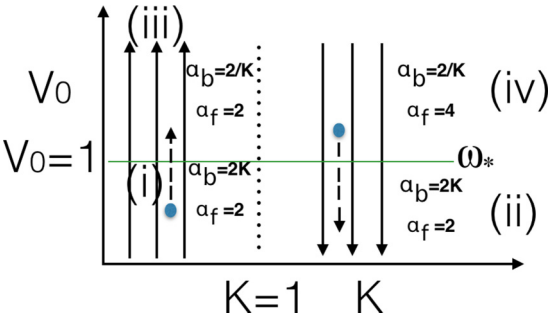

FIG. 2. Various regimes for the energy absorption as a function of the TLL parameter K and the strength of the backscattering potential V_0. The solid line arrows indicate the renormalization flow of the static backscattering potential V_0 [10,11]. For $K < 1$, V_0 flows to the strong coupling limit, and for $K > 1$, V_0 flows to zero. The green line represents the crossover scale ω_* at which the renormalized potential is of order one. α_b and α_f represent the energy deposition exponents corresponding to the backward and forward scattering, respectively (see text). The solid blue circle represents the initial point for the local potential. For $K < 1$, even if the initial point corresponds to a small local potential, it renormalizes to strong coupling when lowering the frequency ω but for $K > 1$, even if the initial point is a large local potential it renormalizes to weak potential via the lowering of ω.

The θ field is not affected by this transformation which preserves the canonical commutation relations (9). In the limit where $\lambda \to 0$ the cosine term is not affected by this transformation since it contains only the value $\phi(x = 0)$. The static Hamiltonian is, thus,

$$H_S = H_0[\tilde{\phi}] + 2V_0\rho_0 \cos(2\tilde{\phi}(0)). \tag{13}$$

The ground state depends crucially on the value of K [10,11]. A renormalization group procedure based on changing the cutoff in the problem (e.g., a high energy cutoff Λ) gives the flow of the parameters,

$$\begin{aligned} \frac{dK}{dl} &= 0, \\ \frac{dV_0}{dl} &= (1 - K)V_0, \end{aligned} \tag{14}$$

where l is the scale of the renormalization for an effective high energy cutoff $\Lambda_l = \Lambda e^{-l}$, Λ is the maximum high energy cutoff, of the order of the bandwidth. Thus for $K > 1$, V_0 flows to 0 and the cosine term is irrelevant. On the other hand for $K < 1$ the cosine is relevant and V_0 flows to the strong coupling limit. A schematic view of the RG flow is shown in Fig. 2.

The redefinition of the field ϕ (12) can also be done in the dynamical terms. Up to terms that are simply oscillating and thus do not contribute to the increase of the average energy (6) one obtains in the limit $\lambda \to 0$,

$$O_V = \delta V\left[-\frac{1}{\pi}\nabla\tilde{\phi}(x = 0) + 2\rho_0 \cos(2\tilde{\phi}(x = 0))\right]. \tag{15}$$

C. Two-component fermionic system

In this section, we consider a two-component fermionic system, given by the Hubbard model. We use similar techniques as for the single-component case. We restrict ourselves for simplicity to the weak coupling case.

The static part of Hamiltonian in bosonized language is given by [5]

$$\begin{aligned} H_S = {} & H_0[\phi_\rho] + H_0[\phi_\sigma] + 2V_0\rho_0 \cos(2\phi_\uparrow(0)) \\ & + 2V_0\rho_0 \cos(2\phi_\downarrow(0)), \end{aligned} \tag{16}$$

$$\begin{aligned} H_S = {} & H_0[\phi_\rho] + H_0[\phi_\sigma] \\ & + 4V_0\rho_0 \cos(\sqrt{2}\phi_\rho(0)) \cos(\sqrt{2}\phi_\sigma(0)), \end{aligned} \tag{17}$$

where $\phi_\uparrow$ and $\phi_\downarrow$ are fields for spin-up and spin-down fermions, $\phi_\rho = \frac{\phi_\uparrow + \phi_\downarrow}{\sqrt{2}}$, $\phi_\sigma = \frac{\phi_\uparrow - \phi_\downarrow}{\sqrt{2}}$, and

$$H_0[\phi_\rho] = \frac{1}{2\pi}\int dx\left[u_\rho K_\rho(\partial_x\theta_\rho(x))^2 + \frac{u_\rho}{K_\rho}(\partial_x\phi_\rho(x))^2\right], \tag{18}$$

$$H_0[\phi_\sigma] = \frac{1}{2\pi}\int dx\left[u_\sigma K_\sigma(\partial_x\theta_\sigma(x))^2 + \frac{u_\sigma}{K_\sigma}(\partial_x\phi_\sigma(x))^2\right]. \tag{19}$$

u_ρ, u_σ, K_ρ, and K_σ are the Luttinger parameters. For a repulsive interaction $K_\rho < 1$ and for a spin rotation symmetric Hamiltonian K_σ renormalizes to $K_\sigma^* = 1$.

The renormalization flow of V_0 is given by [10,11]

$$\frac{dV_0}{dl} = [1 - (K_\sigma + K_\rho)/2]V_0. \tag{20}$$

V_0 is irrelevant for $K_\sigma + K_\rho > 2$, and relevant for $K_\sigma + K_\rho < 2$. The time-dependent part of the Hamiltonian for a weak potential is given by

$$\begin{aligned} O_V = \delta V\Bigg[& -\frac{\sqrt{2}}{\pi}\nabla\phi_\rho(x = 0) \\ & + 4V_0\rho_0 \cos(\sqrt{2}\phi_\rho(0)) \cos(\sqrt{2}\phi_\sigma(0))\Bigg]. \end{aligned} \tag{21}$$

D. Strong coupling

The description of the previous two subsections is well adapted if the potential $V(x,t)$ (and the modulation itself) are weak compared to other parameters in the problem, such as, e.g., the kinetic energy. If the impurity potential V is the largest scale in the problem, then it is more useful to write an effective description using an expansion in powers of $1/V$. We examine such a case for a single-component fermionic system.

In order to do so, we put the system on a lattice and assume that the potential only exists on the site $x = 0$. We also assume that the interactions are onsite and nearest neighbor. We divide the full Hamiltonian in three parts. The first (respectively, second) part contains all sites left (respectively, right) of the origin. The third part is the impurity site. The tunneling and nearest neighbor interaction between sites (kinetic energy) connect the three parts:

$$\begin{aligned} H = {} & H_1 + H_2 - J[\psi_{-1}^\dagger\psi_0 + \psi_1^\dagger\psi_0 + h.c] \\ & + V\psi_0^\dagger\psi_0 + V_n n_0(n_{-1} + n_1). \end{aligned} \tag{22}$$

For a large V we derive the effective Hamiltonian in powers of $1/V$ (see Appendix B). The effective Hamiltonian is

$$H = H_1 + H_2 - \frac{J^2}{V}[(\psi_1^\dagger \psi_{-1} + \text{H.c.}) + \psi_1^\dagger \psi_1 + \psi_{-1}^\dagger \psi_{-1}]. \quad (23)$$

We thus see that the two half parts are coupled by an effective tunneling term,

$$J^{\text{eff}} = \frac{J^2}{V}, \quad (24)$$

and that there is an attractive potential of the same order acting on the last site of each half part.

For the dynamical case we simply assume that we can replace the static V by the dynamical one $V = V_0 + \delta V \cos(\omega t)$, since $V_0 \gg 0$, $1/V = 1/V_0 - \delta V/V_0^2 \cos(\omega t)$. The static part of the Hamiltonian is given by

$$H_S = H_1 + H_2 - J_0[(\psi_{-1}^\dagger(x=-a)\psi_1 + \text{H.c.}) + \psi_1^\dagger \psi_1 + \psi_{-1}^\dagger \psi_{-1}], \quad (25)$$

where 1 and 2 stand for the right and left parts of the one-dimensional chain, $J_0 = J^2/V_0$ and a is the lattice constant.

In this case the amplitude modulation of the potential produces a small modulation of the tunneling amplitude and local potential. The operator O is

$$O = \delta t_1(\psi_1^\dagger(x=-a)\psi_2(x=a) + \text{H.c.}) + \delta t_2(\psi_2^\dagger(x=a) \times \psi_2(x=a) + \psi_1^\dagger(x=-a)\psi_1(x=-a)), \quad (26)$$

where $\delta t_2 = -\frac{\delta V J^2}{V_0^2}$ and $\delta t_1 = -\frac{\delta V J^2}{V_0^2}$. Since J^2/V_0 is small compared to the kinetic energy we can bosonize (23). The expressions are derived in Appendix B, and the final static Hamiltonian is given by

$$H_s = \frac{u}{2\pi}\int_{-\infty}^{\infty} dx[(\partial_x \tilde{\tilde{\theta}}(x))^2 + (\partial_x \tilde{\tilde{\phi}}(x))^2] + \frac{2a\sqrt{K}J^2}{\pi V_0}\partial_x^2 \tilde{\tilde{\theta}}(0) - \frac{2J^2\rho_0}{V_0}\cos\left(\frac{\sqrt{K}}{2}(\tilde{\tilde{\theta}}(a) - \tilde{\tilde{\theta}}(-a))\right) \times \cos\left(\frac{\sqrt{K}}{2}(\tilde{\tilde{\phi}}(a) - \tilde{\tilde{\phi}}(-a))\right) - \frac{2J^2\rho_0}{V_0}\cos\left(\frac{2}{\sqrt{K}}(\tilde{\tilde{\phi}}(0))\right). \quad (27)$$

Note that in (27) there is no "forward scattering" term corresponding to the gradient term in (11). As a result the energy absorption corresponding to the "forward scattering" will be quite different for a weak impurity and a strong one, as discussed below.

III. CALCULATION OF THE ENERGY ABSORPTION

We now compute the energy absorption for the amplitude modulation. Let us consider first the case for which the bare potential is weak as described in Sec. II B.

A. Weak bare potential

If one starts with a weak initial potential both the Hamiltonian and the perturbation are described by (8) and (15) for the single-component case and by (16) and (21) for the two-component one. In the static part of the Hamiltonian the backscattering part of the potential renormalizes as described by (14) and (20). Depending on the value of K (or K_ρ for the two-component case) the potential can either renormalize to zero or flow to strong coupling, leading to a crossover to another regime. If $K > 1$ (respectively, $K_\rho > 1$ for the two-component case) the backscattering term renormalizes to zero, and the energy absorption can thus essentially be computed with the quadratic part of the Hamiltonians (8), (18), and (19). On the contrary if $K < 1$ (respectively, $K_\rho < 1$) the *backscattering* term in (13) and (16) renormalizes to large values. In that case there is a crossover scale below which one cannot ignore the backscattering term in the static Hamiltonian.

We examine sequentially these two cases.

B. Energy deposition in weak coupling limit

To compute the energy absorption rate for the single-component case (15) we use (6) for a Hamiltonian $H = H_0 + \cos(\omega t)(a_1 O_1 + a_2 O_2)$ where, using (15),

$$O_1 = \cos(2\phi(x=0)), \quad (28)$$

$$O_2 = \nabla\phi(x=0). \quad (29)$$

This leads to

$$E_R = -\tfrac{1}{2}a_1^2\omega\text{Im}[\chi_1^R(\omega)] - \tfrac{1}{2}a_2^2\omega\text{Im}[\chi_2^R(\omega)], \quad (30)$$

where $\chi_1^R(t) = -iY(t)\langle[O_1(t), O_1(0)]\rangle_{H_0}$, and $\chi_2^R(t) = -iY(t)\langle[O_2(t), O_2(0)]\rangle_{H_0}$. $Y(t)$ is the Heaviside step function.

The explicit calculation of the correlation is performed in Appendix C and gives

$$E_R = -\frac{1}{2}\left(\frac{\delta V}{\pi}\right)^2\omega\text{Im}[\chi_2^R(\omega)] - \frac{1}{2}(2\delta V\rho_0)^2\omega\text{Im}[\chi_1^R(\omega)] = \frac{\delta V^2 K}{4\pi u^2}\omega^2 + \frac{1}{2}(2\delta V\rho_0)^2\sin(K\pi)\cos(K\pi) \times (u/\alpha)^{-2K}\Gamma(1-2K)\omega^{2K}, \quad (31)$$

where $\chi_1^R(\omega)$ and $\chi_2^R(\omega)$ are defined in (C8) and (C9) of Appendix C, and α is of order of the lattice cutoff.

As we see the energy deposition rate E_R shows a power law behavior as a function of the frequency of the potential modulation. The forward scattering part of the potential leads to an exponent of two, while the backward scattering part has an exponent $2K$. For $K > 1$ the energy deposition rate is dominated at small frequencies by the forward scattering part. Note that the prefactor of the energy absorption gives direct access to the TLL parameters of the system. When $K \to 1$, $\sin(2\pi K)\Gamma(1-2K)$ tends to π and the backward scattering gives also an absorption going as ω^2, a result identical to what would be obtained directly by a free fermion calculation.

For the two-component case, similar calculations lead to

$$E_R = \frac{\delta V^2 K_\rho}{2\pi u_\rho^2}\omega^2 + \frac{1}{2}(4\delta V\rho_0)^2 \sin((K_\rho + K_\sigma)\pi/2) \times \cos((K_\rho + K_\sigma)\pi/2)(u_\rho/\alpha)^{-K_\rho}(u_\sigma/\alpha)^{-K_\sigma} \times \Gamma(1-(K_\rho+K_\sigma))\omega^{K_\rho+K_\sigma}. \quad (32)$$

If $K_\rho > 1$ then the dominant contribution comes also from the forward scattering for small frequencies.

C. Crossover from weak to strong coupling limit and strong to weak coupling limit

The behavior of the previous section remains valid only if one can compute the absorbed energy with the quadratic part of the static Hamiltonian only. This is valid for $K > 1$ or $K_\rho > 1$ since the bare potential of the backscattering term scales down, but becomes incorrect in the opposite limit of $K < 1$ (or $K_\rho < 1$) since in that case the backscattering part scales up in the static Hamiltonian. The RG equations (14) and (20) thus define a scale at which the backscattering term renormalizes to a value of order one, and thus one enters a different regime to compute the absorption. As a function of the frequency of the modulation this defines a crossover frequency ω_* below which the expressions (31) and (32) are not valid any more.

Let us start from a regime where $K < 1$, and a weak bare impurity potential $V_0 < 1$. V_0 will flow to the strong coupling limit by lowering the frequency of the modulation. We can compute the flow parameter l_* at which $V_0(l_*) \simeq \alpha\ \omega_0$. Using (14) we obtain

$$V_0(l_*) = V_0(l=0)\exp[(1-K)l_*] \simeq \alpha\ \omega_0, \quad (33)$$

$$\exp[l_*] = \left(\frac{\alpha\omega_0}{V_0(l=0)}\right)^{\frac{1}{1-K}}. \quad (34)$$

If ω_0 is the maximum frequency cutoff of the order of the bandwidth,

$$\omega_* = \omega_0\left(\frac{\alpha\omega_0}{V_0(l=0)}\right)^{\frac{-1}{1-K}}. \quad (35)$$

In an opposite way, if we had started in the strong coupling regime for which the bare potential of the impurity is very strong as described in Sec. II D but have $K > 1$ the weak tunneling J_0 between the two parts of the chain would flow according to [5,10]

$$\frac{dJ_0}{dl} = [(1-1/K)J_0], \quad (36)$$

leading in a similar way to a crossover scale at which the tunneling becomes of order one,

$$\omega_* = \omega_0\left(\frac{\omega_0}{J_0(l=0)}\right)^{\frac{-1}{1-1/K}}. \quad (37)$$

D. Strong coupling renormalization of backscattering ($K < 1, \omega < \omega_*$)

For frequencies of the modulation $\omega \ll \omega_*$ one enters (for $K < 1$ or $K_\rho < 1$) the strong coupling regime for which the backscattering term plays a central role in the static Hamiltonian. Note that this regime is *a priori* different from the case for which one would have started from a strong bare potential. Indeed in that case both forward and backward scattering would be affected. In the present case the forward scattering potential is not affected in the static part of the Hamiltonian.

To calculate the energy deposition, we use the dilute instanton approximation [5] as described in Appendix D. The energy deposition due to the amplitude modulation in the strong coupling regime is given by

$$E_R = \frac{\delta V^2 K}{4\pi u^2}\omega^2 + \frac{1}{2}M^2(2\delta V\rho_0)^2\cos(\pi/K)\sin(\pi/K) \times \Gamma(1-2/K)(\delta\ \omega)^{2/K}e^{-8\sqrt{2\rho_0 V_0(l_*)}M}, \quad (38)$$

where δ is the short time cutoff. In the dilute instanton calculation, one assumes that the backward scattering potential is very large but near $\omega = \omega_*$, V_0 is not very large. The dilute instanton approximation gives the correct exponent of E_R but does not provide the correct coefficient near ω_*. E_R in the weak coupling and strong coupling limits should match at $\omega = \omega_*$. Using the fact that for $\omega < \omega_*$ one has from (38) $E_R = A(\omega\alpha/u)^{2/K}$ where A is a coefficient to be determined, and for $\omega > \omega_*$ we have (31), the continuity equation reads

$$A(\alpha/u)^{2/K}\omega_*^{2/K} = \sin(K\pi)\cos(K\pi)(u/\alpha)^{-2K} \times \Gamma(1-2K)\omega_*^{2K}, \quad (39)$$

which determined the prefactor A,

$$A = \sin(K\pi)\cos(K\pi) \times (u/\alpha)^{2/K-2K}\Gamma(1-2K)\omega_*^{2K}/(\omega_*)^{2/K} = \sin(K\pi)\cos(K\pi)\quad (u/\alpha)^{2/K-2K}\Gamma(1-2K) \times \omega_0^{2(K-1/K)}(\alpha\omega_0/V_0)^{2(K+1)/K}. \quad (40)$$

At the frequency ω_* the ratio between the part of E_R due to the backward scattering and the one due to the forward scattering is

$$r = \frac{4\pi u^2\rho_0^2\alpha^2\sin(2K\pi)(\alpha\omega_0)^{2K}}{KV_0^2u^{2K}}. \quad (41)$$

Note that for a weak initial potential this ratio can become very large. Thus for frequencies $\omega < \omega_*$ the backward scattering will continue to dominate down to a lower frequency ω_1 below which the energy absorption rate will be dominated by the forward scattering. This frequency is given by

$$\omega = \omega_1 = \left(\frac{\delta V^2 K}{4\pi u^2 A}\right)^{1/(2(1/K-1))}. \quad (42)$$

Note that for $K < 1$ and $\omega > \omega_*$, $\omega < 1$ the energy deposition is still given by (32), and the dominant contribution comes from the backward scattering.

The behavior of the energy deposition is depicted in Fig. 3 for $K < 1$.

E. Strong bare potential

If the impurity potential is very large compared to the kinetic energy or interacting, one needs to start with the

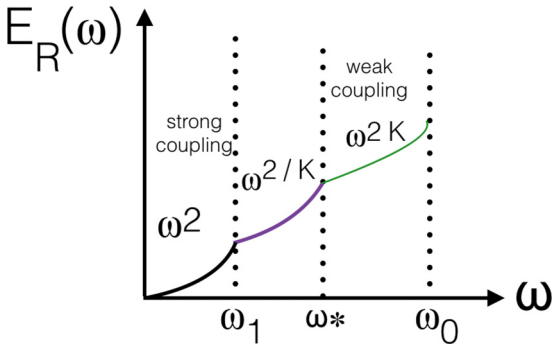

FIG. 3. Energy deposition as a function of frequency for a weak bare potential (see text). Depending on the frequency of the modulation three absorption regimes exist. Above the crossover frequency $\omega = \omega_*$ (dashed line), the backscattering term dominates with a power law absorption ω^{2K}. Between ω_* and ω_1 the backward scattering term dominates with an exponent $2/K$ leading to $\omega^{2/K}$ behavior and below ω_1 absorption is dominated by the forward scattering leading to ω^2 behavior.

Hamiltonian (25) which corresponds to two semi-infinite chains coupled by a hopping term.

The energy modulation is thus given by

$$E_R = \frac{\delta t_3^2 \pi}{4u^4}\omega^4 + \frac{1}{2}(\delta t_4)^2 \cos(\pi/K)\sin(\pi/K) \times \Gamma(1-2/K)(u/\alpha)^{-2/K}\omega^{2/K}, \quad (43)$$

where $\delta t_3 = -\frac{2a\sqrt{K}\delta V J^2}{\pi V_0^2}$ and $\delta t_4 = \frac{2J^2\delta V \rho_0}{V_0^2}$, a is the lattice spacing, and J the tunneling.

The energy deposition rate shows again a power law behavior. The exponent is the same as the one corresponding to the renormalized backward scattering, discussed in the previous section. Note, however, that the part corresponding to the forward scattering is now different. In this case the forward scattering contributes to an absorption going as ω^4 instead of ω^2 for a weak potential and thus the energy absorption is dominated by the *backscattering* potential, as long as $0.5 < K < 1$. When $K < 0.5$ the system is again dominated by the absorption coming from the forwards scattering.

In the case $K > 1$ the tunneling between the two half systems will scale up as described by the flow equation (36). There is thus again a scale ω_* at which the tunneling becomes of order one and then the Hamiltonian switches back to the one with a weak backscattering term. In that case the exponent becomes similar to the one obtained in Sec. III B and is $2K$. So for $1 < K < 2$ the backscattering absorption dominates as very small frequencies, while the forward scattering dominates for $K > 2$.

Note that since the prefactors in the strong coupling limit for both backward and forward scattering are proportional to $1/V_0^2$, the energy deposition will be very small in comparison to the weak coupling case.

IV. RESULTS AND DISCUSSION

Our results show that the time-dependent modulation of a single impurity in an interacting bath of bosons or fermions allows one to probe the TLL nature of the bath, the frequency of the modulation, and the interactions between particles serving as control parameters. Each regime is essentially characterized by a power law behavior of the absorbed energy. As detailed in the previous sections the precise power depends on (i) the forward and the backward scattering parts of the impurity potential; (ii) the initial strength of the impurity potential compared to the energy scales of the bath Hamiltonian; (iii) the value of the interactions between the particles in the bath. The results are summarized in Fig. 2.

Experiments in ultracold gases would thus be prime candidates to test the effects predicted here. Indeed several experiments with bulk modulation of the amplitude of the optical lattices have already shown [18,19,28] the interest of this technique. We here propose to do this modulation locally. Since the modulation is local this has the advantage to be less sensitive to perturbations such as a confining harmonic potential. On the other hand the effect of the perturbation is now much smaller of the order of $1/L$ where L is the size of the system, and thus more difficult to measure.

Let us discuss separately the two cases of bosons and fermions.

A. Bosonic systems

Realizing interacting one-dimensional bosonic systems in which modulation is possible has been already demonstrated [18,21]. Putting a local potential is possible either with a light blade [29] or in boson microscopes by locally addressing a single site [30]. Measurement of the energy deposited in the system can be obtained either by measuring the momentum distribution [18] or in a microscope by looking at the number fluctuations [30]. Especially in the last case, realizing box potentials should also be possible.

For bosons with local interactions we have $K > 1$ and thus are on the right part of Fig. 2. A weak potential should thus show an absorption dominated by the forward scattering potential, scaling essentially as ω^2. It could be interesting if feasible to engineer a local potential so that the forward part of the potential would be much smaller than the backward one. For example, for a system with one boson every two sites would require a potential of the form V_0 on $x = -1$ and $-V_0$ on $x = 0$. This would reinforce strongly the backscattering part and thus show the ω^{2K} absorption that would correspond to this component of the potential.

Alternatively one could get rid of the forward scattering component by going to a very strong on-site potential as detailed in Sec. II D. In such a case one would start with absorption scaling as $\omega^{2/K}$ which for weakly repulsive bosons for which K can be large would correspond to a nearly constant absorption rate. At the crossover ω_* the absorption would drop brutally since it would behave as ω^{2K}. The crossover scale ω_* corresponding to the renormalization of the potential in the *static* part, should thus be visible with this method.

B. Fermionic systems

Shaking in fermionic systems has already been used for Hubbard-like Hamiltonians [28]. Instead of measuring the deposited energy, the growth of double occupancy allows for a more sensitive detection technique [24,25,28]. Fermionic

systems allow also potentially to reach the regime $K < 1$. However, single-component fermionic systems would require one to have also finite range interactions which is for the moment still not too common in experiments. Reaching such a regime with long-range interactions can of course be also done with bosonic systems. For fermions it is, however, simpler to use two-component systems. In particular recent experiments have demonstrated the possibility to have fermionic microscopes [26,27,31] in which such two-component fermionic systems can be manipulated. These experiments would be ideal test beds for the effects described in the previous sections.

One could then explore potentially the same effects as the ones for bosons, namely the scaling ω^{2K} and $\omega^{2/K}$ of the absorbed energy. In particular for a very large repulsion U and a weak bare local potential one would expect an absorption $E_R \sim \omega^{3/2}$ since the limit of the exponent K_ρ for the Hubbard model is $K_\rho = 1/2$.

V. CONCLUSION

In this work, we have studied the energy deposition due to the periodic modulation in time of a local potential in an interacting one-dimensional system of bosons or fermions. Using linear response and bosonization we have computed the absorbed energy both for the regimes of a weak and a strong local potential. We find an absorption varying as a power law of the modulating frequency, with exponents that depend both on the interactions in the system and the nature and strength of the local potential. The results are summarized in Fig. 2. This behavior allows one to probe the TLL nature of the one-dimensional interacting systems and we have discussed the experimental consequences of potential experiments in ultracold gases.

Quite generally this study shows the possibility of engineering local time-dependent potentials, and allows one to use the frequency of the modulation probe as a scale to explore the various renormalization regimes that the local potential would lead to. The advantage of the technique is that the modulation frequency can be precisely controlled in a large range of scales. The drawback is clearly that the measurement of the energy deposited is an effect varying as the inverse size of the system and thus difficult to measure. One could thus replace such a measurement by measurements of the *local* density, which could potentially be achieved in systems such as the microscopes. Studies along that line are under way.

ACKNOWLEDGMENTS

We would like to thank I. Bloch for interesting discussions. This work is supported by the Swiss National Science Foundation under MaNEP and Division II.

APPENDIX A: LINEAR RESPONSE

We give here a brief reminder of the energy deposition in a system by a periodic modulation of the form (4) The rate of energy deposition in a system of Hamiltonian $H = H_0 + a_0 \cos(\omega t) O$, is given by

$$\dot{E} = \frac{\partial \bar{H}}{\partial t} = -\omega a_0 \sin(\omega t) \overline{O(x=0,t)}, \tag{A1}$$

where H_0 is a static part of the Hamiltonian, a_0 is the amplitude of the time-dependent oscillation $\cos(\omega t)$, and O is an operator coupled to the time-dependent oscillation $\cos(\omega t)$, within LRT, $\bar{O}$ is given by

$$\overline{O(t)} = \langle O(t)\rangle_{H_0} - i a_0 \int_0^\infty dt_1 \cos(\omega(t-t_1)) \times \langle [O(t_1), O(0)]\rangle_{H_0}. \tag{A2}$$

By using (A2), $\overline{O}$ is given by

$$\begin{aligned} \overline{O(t)} &= \langle O(t)\rangle_{H_0} - i a_0 \int_0^\infty dt_1 \cos(\omega(t-t_1)) \times \langle [O(t_1), O(0)]\rangle_{H_0}, \\ \overline{O(t)} &= \langle O(t)\rangle_{H_0} + a_0 \int_0^\infty dt_1 \cos(\omega(t-t_1)) X^R(t_1), \\ \overline{O(t)} &= \langle O(t)\rangle_{H_0} + \frac{a_0}{2}[e^{i\omega t}\chi^R(-\omega) + e^{-i\omega t}\chi^R(\omega)], \end{aligned} \tag{A3}$$

where $\chi^R(t) = -iY(t)\langle [O(t), O(0)]\rangle_{H_0}$ and $Y(t)$ is the Heaviside step function.

By using (A3), (A1) can be expressed as

$$\dot{E}(t) = -\omega a_0 \sin(\omega t)\langle O(t)\rangle_{H_0} - \tfrac{1}{2} a_0^2 \omega \sin(\omega t)[e^{i\omega t}\chi^R(-\omega) + e^{-i\omega t}\chi^R(\omega)]. \tag{A4}$$

We now calculate the cycle average of $\dot{E}(t)$ over the period $T = 2\pi/\omega$.

$$\begin{aligned} E_R &= \frac{1}{T}\int_0^T dt \dot{E}(t) \\ &= -\frac{1}{4i} a_0^2 \omega \big[-\chi_2^R(-\omega) + \chi^R(\omega)\big] \\ &= -\frac{1}{2} a_0^2 \omega \mathrm{Im}[\chi^R(\omega)]. \end{aligned} \tag{A5}$$

APPENDIX B: EFFECTIVE HAMILTONIAN FOR LARGE V

In this section, we derive the effective Hamiltonian for a system of hard core bosons for a large V, in the power of $1/V$. We consider, the site at $x = 0$ is connected to sites at $x = -1$ and $x = 1$ via tunneling J, and nearest neighbor interaction V_n.

$$H = H_1 + H_2 + H_3, \tag{B1}$$

where, H_1 and H_2 represent the left and right parts of the Hamiltonian. H_3 is given by

$$H_3 = -J[\psi_{-1}^\dagger \psi_0 + \psi_1^\dagger \psi_0 + h.c] + V \psi_0^\dagger \psi_0 + V_n n_0 (n_{-1} + n_1). \tag{B2}$$

H_3 in the basis of $|0,0,0\rangle,|0,1,0\rangle,|0,0,1\rangle,|1,0,0\rangle,|1,1,0\rangle,|1,0,1\rangle|0,1,1\rangle,|1,1,1\rangle$ is expressed as

$$H_3 = \begin{bmatrix} 0 & 0 & 0 & 0 & 0 & 0 & 0 & 0 \\ 0 & V & -J & -J & 0 & 0 & 0 & 0 \\ 0 & -J & 0 & 0 & 0 & 0 & 0 & 0 \\ 0 & -J & 0 & 0 & 0 & 0 & 0 & 0 \\ 0 & 0 & 0 & 0 & V+V_n & -J & 0 & 0 \\ 0 & 0 & 0 & 0 & -J & 0 & -J & 0 \\ 0 & 0 & 0 & 0 & 0 & -J & V+V_n & 0 \\ 0 & 0 & 0 & 0 & 0 & 0 & 0 & V+2V_n \end{bmatrix}. \tag{B3}$$

H_3 is composed of two block diagonal matrices depending on the total number of particles. We examine the part with one particle and two particles.

$$\tilde{H} = \begin{bmatrix} V & -J & -J & 0 & 0 & 0 \\ -J & 0 & 0 & 0 & 0 & 0 \\ -J & 0 & 0 & 0 & 0 & 0 \\ 0 & 0 & 0 & V+V_n & -J & 0 \\ 0 & 0 & 0 & -J & 0 & -J \\ 0 & 0 & 0 & 0 & -J & V+V_n \end{bmatrix}. \tag{B4}$$

$\tilde{H} = \tilde{H}_t + \tilde{H}_V$, where $\tilde{H}_t$ contains only tunneling, and $\tilde{H}_V = \tilde{H} - \tilde{H}_t$. In order to find the low energy effective Hamiltonian, we make a canonical transformation of $\tilde{H}$.

$$\overline{H} = W\tilde{H}W^\dagger \simeq \left(1 + i\tilde{S} + \frac{(i)^2}{2}\tilde{S}^2\right)\tilde{H}\left(1 - i\tilde{S} + \frac{(-i)^2}{2}\tilde{S}^2\right) \simeq \tilde{H} + i[\tilde{S},\tilde{H}] + \frac{i^2}{2}[\tilde{S},[\tilde{S},\tilde{H}]] + O(\tilde{S}^3).$$

where $W = e^{i\tilde{S}}$. The canonical transformation does not change the eigenvalues of the Hamiltonian but rotates the eigenstate $|\psi\rangle$ to $e^{i\tilde{S}}|\psi\rangle$ and we chose $\tilde{S}$ such that $\tilde{H}_t + i[\tilde{S},\tilde{H}_V] = 0$,

$$\tilde{S} = \begin{bmatrix} 0 & \frac{iJ}{V} & \frac{iJ}{V} & 0 & 0 & 0 \\ -\frac{iJ}{V} & 0 & 0 & 0 & 0 & 0 \\ -\frac{iJ}{V} & 0 & 0 & 0 & 0 & 0 \\ 0 & 0 & 0 & 0 & \frac{iJ}{V_n+V} & 0 \\ 0 & 0 & 0 & \frac{-iJ}{V_n+V} & 0 & \frac{-iJ}{V_n+V} \\ 0 & 0 & 0 & 0 & \frac{iJ}{V_n+V} & 0 \end{bmatrix}, \tag{B5}$$

$$\overline{H} = \tilde{H}_1 \oplus \tilde{H}_2, \tag{B6}$$

$$\overline{H} = \begin{bmatrix} \frac{2J^2}{V}+V & \frac{4J^3}{V^2} & \frac{4J^3}{V^2} & 0 & 0 & 0 \\ \frac{4J^3}{V^2} & \frac{-J^2}{V} & \frac{-J^2}{V} & 0 & 0 & 0 \\ \frac{4J^3}{V^2} & \frac{-J^2}{V} & \frac{-J^2}{V} & 0 & 0 & 0 \\ 0 & 0 & 0 & d+\frac{J^2}{V_n+V} & \frac{4J^3}{(V_n+V)^2} & \frac{J^2}{V_n+V} \\ 0 & 0 & 0 & \frac{4J^3}{(V_n+V)^2} & \frac{-2J^2}{V_n+V} & \frac{4J^3}{(V_n+V)^2} \\ 0 & 0 & 0 & \frac{J^2}{V_n+V} & \frac{4J^3}{(V_n+V)^2} & d+\frac{J^2}{V_n+V} \end{bmatrix}, \tag{B7}$$

where $d = V_n + V$.

$$\tilde{H}_1 = \begin{bmatrix} \frac{2J^2}{V}+V & \frac{4J^3}{V^2} & \frac{4J^3}{V^2} \\ \frac{4J^3}{V^2} & \frac{-J^2}{V} & \frac{-J^2}{V} \\ \frac{4J^3}{V^2} & \frac{-J^2}{V} & \frac{-J^2}{V} \end{bmatrix}, \tag{B8}$$

$$\tilde{H}_2 = \begin{bmatrix} V_n+V+\frac{J^2}{V_n+V} & \frac{4J^3}{(V_n+V)^2} & \frac{J^2}{V_n+V} \\ \frac{4J^3}{(V_n+V)^2} & \frac{-2J^2}{V_n+V} & \frac{4J^3}{(V_n+V)^2} \\ \frac{J^2}{V_n+V} & \frac{4J^3}{(V_n+V)^2} & V_n+V+\frac{J^2}{V_n+V} \end{bmatrix}. \tag{B9}$$

Since V is very large, hence $1/V^2 \simeq 0$,

$$\tilde{H}_1 \simeq \begin{bmatrix} \frac{2J^2}{V}+V & 0 & 0 \\ 0 & \frac{-J^2}{V} & \frac{-J^2}{V} \\ 0 & \frac{-J^2}{V} & \frac{-J^2}{V} \end{bmatrix}, \tag{B10}$$

$$\tilde{H}_2 = \begin{bmatrix} V_n+V+\frac{J^2}{V_n+V} & 0 & \frac{J^2}{V_n+V} \\ 0 & \frac{-2J^2}{V_n+V} & 0 \\ \frac{J^2}{V_n+V} & 0 & V_n+V+\frac{J^2}{V_n+V} \end{bmatrix}. \tag{B11}$$

In the original Hamiltonian (B3), the $n_0 = 0$ sector is coupled to $n_0 = 1$ sector via J but after the canonical transformation the $n_0 = 0$ sector is completely decoupled from the $n_0 = 1$ sector. The sector $n_0 = 0$ represents the low energy effective Hamiltonian. It is thus given by

$$\overline{H} = -\frac{J^2}{V}[|100\rangle\langle 100| + |001\rangle\langle 001| + |100\rangle\langle 001| + |001\rangle\langle 100| - \frac{2J^2}{V+V_n}|101\rangle\langle 101|]. \tag{B12}$$

The full low energy Hamiltonian is thus

$$H = H_1 + H_2 - \frac{J^2}{V}[|100\rangle\langle 100| + |001\rangle\langle 001| + |100\rangle\langle 001| + |001\rangle\langle 100| - \frac{2J^2}{V+V_n}|101\rangle\langle 101|]. \tag{B13}$$

In second quantization (B13) can be written as

$$H = H_1 + H_2 + b(\psi_1(-a)^\dagger\psi_2(a) + h.c) - c(n_1(-a) + n_2(a)) + \tilde{V}_n n_1(-a)n_2(a). \tag{B14}$$

Using (B13) and (B14) we find $b = -\frac{J^2}{V}$, $c = \frac{J^2}{V}$, $\tilde{V}_n - 2c = -\frac{2J^2}{V+V_n}, \tilde{V}_n \simeq 0$.

The bosonized form of H is given by

$$\begin{aligned} H = {} & \frac{1}{2\pi}\int_{-\infty}^{0} dx\Big[uK(\partial_x\theta_1(x))^2 + \frac{u}{K}(\partial_x\phi_1(x))^2\Big] + \frac{1}{2\pi}\int_{0}^{\infty} dx\Big[uK(\partial_x\theta_2(x))^2 + \frac{u}{K}(\partial_x\phi_2(x))^2\Big] \\ & + \frac{J^2}{\pi V}\partial_x\phi_1(-a) + \frac{J^2}{\pi V}\partial_x\phi_2(a) - \frac{2J^2\rho_0}{V}(\cos(2\phi_1(-a)) + \cos(2\phi_2(a))) - \frac{2J^2\rho_0}{V}\cos(\theta_1(-a) - \theta_2(a)). \end{aligned} \tag{B15}$$

At $x = 0$, the number of particles is zero, which is imposed by $\phi_1(0) = \phi_2(0) = 0$. Now let us define H as

$$H = H_{10} + H_{20} + \frac{J^2}{\pi V}\partial_x\phi_1(-a) + \frac{J^2}{\pi V}\partial_x\phi_2(a) - \frac{2J^2\rho_0}{V}(\cos(2\phi_1(-a)) - \cos(2\phi_2(a))) - \frac{2J^2\rho_0}{V}\cos(\theta_1(-a) - \theta_2(a)), \tag{B16}$$

where $H_{10} = \frac{1}{2\pi}\int_{-\infty}^{0} dx[uK(\partial_x\theta_1(x))^2 + \frac{u}{K}(\partial_x\phi_1(x))^2]$ and $H_{20} = \frac{1}{2\pi}\int_{0}^{\infty} dx[uK(\partial_x\theta_2(x))^2 + \frac{u}{K}(\partial_x\phi_2(x))^2]$.

We define the fields $\theta = \frac{\tilde{\theta}}{\sqrt{K}}$ and $\phi = \sqrt{K}\tilde{\phi}$. Using these fields H_{10} and H_{20} can be written as

$$H_{10} = \frac{1}{2\pi}\int_{-\infty}^{0} dx[u(\partial_x\tilde{\theta}_1(x))^2 + u(\partial_x\tilde{\phi}_1(x))^2], \tag{B17}$$

and

$$H_{20} = \frac{1}{2\pi}\int_{0}^{\infty} dx[u(\partial_x\tilde{\theta}_2(x))^2 + u(\partial_x\tilde{\phi}_2(x))^2]. \tag{B18}$$

Define $\tilde{\phi},\tilde{\theta}$ in terms of the chiral fields $\tilde{\phi}_L = \tilde{\phi} + \tilde{\theta}, \tilde{\phi}_R = \tilde{\theta} - \tilde{\phi}$; the constraint $\phi_1(0) = \phi_2(0) = 0$ is fixed by $\tilde{\phi}_L(x) = \tilde{\phi}_R(-x)$ [5]. H_{10} and H_{20} are expressed in terms of the new fields $\tilde{\phi}_L$ and $\tilde{\phi}_R$ by

$$H_{10} = \frac{u}{4\pi}\int_{-\infty}^{\infty} dx(\partial_x\tilde{\phi}_{R1}(x))^2, \quad H_{20} = \frac{u}{4\pi}\int_{-\infty}^{\infty} dx(\partial_x\tilde{\phi}_{L2}(x))^2. \tag{B19}$$

In terms of $\tilde{\phi}_{R1}$ and $\tilde{\phi}_{L2}$, $\partial_x\phi_1(-a) + \partial_x\phi_2(a)$ becomes as

$$\begin{aligned} \partial_x(\phi_1(-a) + \phi_2(a)) &= \sqrt{K}\partial_x[\tilde{\phi}_1(-a) + \tilde{\phi}_2(a)] = \frac{\sqrt{K}}{2}\partial_x[\tilde{\phi}_{L1}(-a) - \tilde{\phi}_{R1}(-a) + \tilde{\phi}_{L2}(a) - \tilde{\phi}_{R2}(a)] \\ &= \frac{\sqrt{K}}{2}\partial_x[\tilde{\phi}_{R1}(a) - \tilde{\phi}_{R1}(-a) + \tilde{\phi}_{L2}(a) - \tilde{\phi}_{L2}(-a)] \simeq \frac{\sqrt{K}}{2}2a\partial_x[\partial_x\tilde{\phi}_{R1}(0) + \partial_x\tilde{\phi}_{L2}(0)] \\ &= a\sqrt{K}\partial_x[\partial_x\tilde{\phi}_{R1}(0) + \partial_x\tilde{\phi}_{L2}(0)]. \end{aligned} \tag{B20}$$

In the same way,

$$\cos(\theta_1(-a)-\theta_2(a)) = \cos\left(\frac{1}{\sqrt{K}}(\tilde{\theta}_1(-a)-\tilde{\theta}_2(a))\right) = \cos\left(\frac{1}{2\sqrt{K}}(\tilde{\phi}_{L1}(-a)+\tilde{\phi}_{R1}(-a)-\tilde{\phi}_{L2}(a)-\tilde{\phi}_{R2}(a))\right)$$
$$\simeq \cos\left(\frac{1}{\sqrt{K}}(\tilde{\phi}_{R1}(0)-\tilde{\phi}_{L2}(0))\right), \tag{B21}$$

and

$$\cos(\phi_1(-a)) = \cos\left(\frac{\sqrt{K}}{2}(\tilde{\phi}_{R1}(a)-\tilde{\phi}_{R1}(-a))\right), \quad \cos(\phi_2(a)) = \cos\left(\frac{\sqrt{K}}{2}(\tilde{\phi}_{L2}(a)-\tilde{\phi}_{L2}(-a))\right). \tag{B22}$$

Finally we define new fields $\tilde{\tilde{\theta}} = \frac{\tilde{\phi}_{R1}+\tilde{\phi}_{L2}}{2}$ and $\tilde{\tilde{\phi}} = \frac{\tilde{\phi}_{L2}-\tilde{\phi}_{R1}}{2}$, and by using (B19)–(B22), the Hamiltonian (B16) can be written as

$$H = \frac{u}{2\pi}\int_{-\infty}^{\infty} dx[(\partial_x\tilde{\tilde{\theta}}(x))^2+(\partial_x\tilde{\tilde{\phi}}(x))^2] + \frac{2a\sqrt{K}J^2}{\pi V}\partial_x^2\tilde{\tilde{\theta}}(0) - \frac{2J^2\rho_0}{V}\cos\left(\frac{\sqrt{K}}{2}(\tilde{\tilde{\theta}}(a)-\tilde{\tilde{\theta}}(-a))\right)$$
$$\times \cos\left(\frac{\sqrt{K}}{2}(\tilde{\tilde{\phi}}(a)-\tilde{\tilde{\phi}}(-a))\right) - \frac{2J^2\rho_0}{V}\cos\left(\frac{2}{\sqrt{K}}(\tilde{\tilde{\phi}}(0))\right). \tag{B23}$$

Since $V = V_0 + \delta V\cos(\omega t)$, and $V_0 \gg \delta V$, this means that $1/V = 1/V_0(1-\delta V/V_0\cos(\omega t)) = 1/V_0 - \delta V/V_0^2\cos(\omega t)$.

APPENDIX C: CALCULATION OF CORRELATION FUNCTIONS

In this section, we compute response functions that are useful to obtain the energy deposition in the system. Two types of correlation functions are required and denoted by $\chi_1^R(\omega)$ and $\chi_2^R(\omega)$. These correlation functions are defined below.

$$\chi_1(\tau) = -\langle T_\tau\cos(2\phi(\tau))\cos(2\phi(0))\rangle_{H_0} = -\langle T_\tau\sin(2\phi(\tau))\sin(2\phi(0))\rangle_{H_0} = -\tfrac{1}{2}\langle T_\tau e^{2i\phi(\tau)}e^{-2i\phi(0)}\rangle_{H_0}$$
$$= -\tfrac{1}{2}e^{-2K\log(u|\tau|/\alpha)} = -\tfrac{1}{2}(u|\tau|/\alpha)^{-2K}, \tag{C1}$$

where T_τ is the time ordering operator, $\tau = it$ is imaginary time, and t is real time.

Correlation function $\chi_1(\tau)$ in real time is given by

$$\chi_1^T(t) = -\tfrac{1}{2}(uit/\alpha)^{-2K} = -\tfrac{1}{2}(i)^{-2K}(ut/\alpha)^{-2K} = -\tfrac{1}{2}(ut/\alpha)^{-2K}(\cos(\pi K) - i\sin(\pi K)). \tag{C2}$$

The retarded correlation function in real time is defined as

$$\chi_1^R(t) = -iY(t)\langle[\cos(2\phi(t)),\cos(2\phi(0))]\rangle_{H_0} = -Y(t)\big[2\mathrm{Im}\chi_1^T(t)\big] = -Y(t)\sin(\pi K)(ut/\alpha)^{-2K}. \tag{C3}$$

1. Fourier transformation of $\chi^R(t)$

Fourier transformation of $\chi_1^R(t)$ is expressed as

$$\chi_1^R(\omega) = \int_{-\infty}^{\infty} dt\; e^{i\omega t}\chi^R(t) = -\int_0^{\infty} dt\; e^{i\omega t}\sin(\pi K)(ut/\alpha)^{-2K}. \tag{C4}$$

The above integral can be evaluated as

$$\int_0^{\infty} dt\; e^{i\omega t}\sinh(\pi t/\beta)^{-2K} = 2^{2K}\frac{\beta}{2\pi}B\left(\frac{-i\beta\omega}{2\pi}+K,1-2K\right). \tag{C5}$$

As $\beta\to\infty$, $\sinh(\pi t/\beta) = \pi t/\beta \Rightarrow \beta/\pi\sinh(\pi t/\beta) = t$,

$$\int_0^{\infty} dt\; e^{i\omega t}(\beta/\pi)^{-2K}\sinh(\pi t/\beta)^{-2K} = 2^{2K-1}\left(\frac{\beta}{\pi}\right)^{-2K+1}B\left(\frac{-i\beta\omega}{2\pi}+K,1-2K\right). \tag{C6}$$

Equation (C5) can be expressed as

$$\int_0^{\infty} dt\; e^{i\omega t}(t)^{-2K} = 2^{2K-1}\left(\frac{\beta}{\pi}\right)^{-2K+1}B\left(\frac{-i\beta\omega}{2\pi}+K,1-2K\right) \simeq 2^{2K-1}\left(\frac{\beta}{\pi}\right)^{-2K+1}\Gamma(1-2K)$$
$$\left(\frac{-i\beta\omega}{2\pi}\right)^{2K-1} = (-i\omega)^{2K-1}\Gamma(1-2K) = e^{-i\pi(K-1/2)}\Gamma(1-2K)\omega^{2K-1}. \tag{C7}$$

Equation (C4) can be written as

$$\chi_1^R(\omega) = -\sin(\pi K)(u/\alpha)^{-2K} e^{-i\pi(K-1/2)}\,\Gamma(1-2K)\omega^{2K-1},$$
$$\mathrm{Im}\big[\chi_1^R(\omega)\big] = \sin(\pi K)(u/\alpha)^{-2K}\sin(\pi(K-1/2))\Gamma(1-2K)\omega^{2K-1}. \tag{C8}$$

Response function of $\partial_x\phi(0,0)$ is given by

$$\chi_2^R(t) = -iY(t)\langle[\partial_x\phi(0,t),\partial_x\phi(0,0)]\rangle_{H_0}, \quad \chi_2^R(\omega) = -\frac{uK}{2}\int dk\frac{k^2}{-(\omega+i\delta)^2+(uk)^2},$$
$$\mathrm{Im}\big[\chi_2^R(\omega)\big] = -\frac{uK\pi}{4\omega}\int dk k^2\delta\left(\frac{-\omega^2+(uk)^2}{2\omega}\right), \quad \mathrm{Im}\big[\chi_2^R(\omega)\big] = -\frac{K\pi\omega}{2u^2}. \tag{C9}$$

APPENDIX D: CALCULATION OF CORRELATION FUNCTIONS WHEN V_0 IS RELEVANT ($K < 1$)

In this section, we will derive the two-point correlation function $\langle\phi(q_1)\phi(q_2)\rangle$ in terms of a local field $\phi(0,\tau)$. We define the local field $\phi_0(\tau)$, acting at $x = 0$ as

$$\phi(0,\tau) = \phi_0(\tau). \tag{D1}$$

By using (D1), $R(q_1,q_2) = \langle\phi(q_1)\phi(q_2)\rangle$ can be written as

$$R(q_1,q_2) = \frac{\int \mathcal{D}\phi\mathcal{D}\phi_0\mathcal{D}\lambda\phi(q_1)\phi(q_2)e^{(-S-i\int d\tau\lambda(\tau)[\phi_0(\tau)-\phi(0,\tau)])}}{\int \mathcal{D}\phi\mathcal{D}\phi_0\mathcal{D}\lambda e^{(-S-i\int d\tau\lambda(\tau)[\phi_0(\tau)-\phi(0,\tau)])}}. \tag{D2}$$

S is the action of the system, and λ is a Lagrange multiplier. Now define $-S - i\int d\tau\lambda(\tau)[\phi_0(\tau)-\phi(0,\tau)]$ in terms of the frequency (ω) and momentum (k).

$$\begin{aligned} I = S + i\int d\tau\lambda(\tau)[\phi_0(\tau)-\phi(0,\tau)] &= \frac{1}{2\pi Ku}\frac{1}{\beta\Omega}\sum_q\left(\omega_n^2+u^2k^2\right)\phi^*(q)\phi(q) \\ &+ i\left[\frac{1}{\beta}\sum_{\omega_n}\lambda^*(\omega_n)\phi_0(\omega_n) - \frac{1}{\beta\Omega}\sum_q\lambda^*(\omega_n)\phi(q)\right] + 2V_0\rho_0\int d\tau\cos(2\phi_0(\tau)) \\ = \frac{1}{2\pi Ku}\frac{1}{\beta\Omega}\sum_q\left(\omega_n^2+u^2k^2\right)&(\phi^*(q) - \frac{i\pi uK}{\left(\omega_n^2+u^2k^2\right)}\lambda^*(\omega_n))(\phi(q) - \frac{i\pi uK}{\left(\omega_n^2+u^2k^2\right)}\lambda(\omega_n)) + \frac{\pi K}{4\beta}\sum_{\omega_n}\frac{1}{|\omega_n|}(\lambda^*(\omega_n) \\ &+ \frac{2i|\omega_n|}{\pi K}\phi_0^*(\omega_n))(\lambda(\omega_n) + \frac{2i|\omega_n|}{\pi K}\phi_0(\omega_n)) + \frac{1}{\beta}\sum_{\omega_n}\frac{|\omega_n|}{\pi K}\phi_0^*(\omega_n)\phi_0(\omega_n) + 2V_0\rho_0\int d\tau\cos(2\phi_0(\tau)). \end{aligned} \tag{D3}$$

By using (D3) and (D2) can be written as

$$\begin{aligned} R(q_1,q_2) = \frac{\pi K\beta\Omega u}{\omega_{n_1}^2+u^2k_1^2}\delta_{q_1,-q_2} &- \frac{\pi^2u^2K^2}{\left(\omega_{n_1}^2+u^2k_1^2\right)\left(\omega_{n_2}^2+u^2k_2^2\right)}\frac{2\beta|\omega_{n_1}|}{\pi K}\delta_{\omega_{n_1},-\omega_{n_2}} + \frac{\pi^2u^2K^2}{\left(\omega_{n_1}^2+u^2k_1^2\right)\left(\omega_{n_2}^2+u^2k_2^2\right)}\frac{4|\omega_{n_1}||\omega_{n_2}|}{\pi^2K^2} \\ &\times\frac{\int\mathcal{D}\phi_0\phi_0(\omega_{n_1})\phi_0(\omega_{n_2})e^{-\frac{1}{\beta\pi K}\sum_{\omega_n}|\omega_n|\phi_0^*(\omega_n)\phi_0(\omega_n)-S_I}}{\int\mathcal{D}\phi_0 e^{-\frac{1}{\beta\pi K}\sum_{\omega_n}|\omega_n|\phi_0^*(\omega_n)\phi_0(\omega_n)-S_I}}, \end{aligned} \tag{D4}$$

where $S_I = 2V_0\rho_0\int d\tau\cos(2\phi_0(\tau))$

$$-\langle\nabla\phi(0,\tau)\nabla\phi(0,0)\rangle = -\left(\frac{1}{\beta\Omega}\right)^2\sum_{q_1,q_2}(-k_1k_2)e^{(-i\omega_{n_1}\tau)}\langle\phi(q_1)\phi(q_2)\rangle. \tag{D5}$$

By using (D4), (D5) can be written as

$$-\langle\nabla\phi(0,\tau)\nabla\phi(0,0)\rangle = -\left(\frac{1}{\beta\Omega}\right)^2\sum_{q_1,q_2}(-k_1k_2)e^{(-i\omega_{n_1}\tau)}\frac{\pi K\beta\Omega u}{\omega_{n_1}^2+u^2k_1^2}\delta_{q_1,-q_2}. \tag{D6}$$

Fourier transformation of (D6) can be written as

$$-\langle\nabla\phi(0,\tau)\nabla\phi(0,0)\rangle(\omega_n) = -\left(\frac{1}{\Omega}\right)\sum_k(k^2)\frac{\pi Ku}{\omega_n^2+u^2k^2}, \quad -\mathrm{Im}(\langle\nabla\phi(0,\tau)\nabla\phi(0,0)\rangle(\omega)) = -\frac{K\pi\omega}{2u^2}. \tag{D7}$$

1. Dilute instanton approximation

By using (D3), the effective action in terms of the local field ϕ_0 is given by

$$S = \frac{1}{\beta\pi K}\sum_{\omega_n}|\omega_n|\phi_0^*(\omega_n)\phi_0(\omega_n) + 2V_0\rho_0\int d\tau\cos(2\phi_0(\tau)). \tag{D8}$$

The action diverges for the large frequency, and to overcome this problem, we add a mass term $\frac{1}{2}M(\partial_\tau\phi)^2$[5,10] to the action.

$$S = \frac{1}{\beta\pi K}\sum_{\omega_n}|\omega_n|\phi_0^*(\omega_n)\phi_0(\omega_n) + 2V_0\rho_0\int d\tau\cos(2\phi_0(\tau)) + \int d\tau\frac{1}{2}M(\partial_\tau\phi)^2. \tag{D9}$$

For a very large V_0, the partition function is dominated by a trajectory, which minimizes the action $2V_0\rho_0\int d\tau\cos(2\phi_0(\tau)) + \int d\tau\frac{1}{2}M(\partial_\tau\phi)^2$, and solution is given by [5,11]

$$\frac{M}{2}\left(\frac{d\phi(\tau)}{d\tau}\right)^2 = \cos(2\phi(\tau)) - 1, \tag{D10}$$

$$\tilde{\phi}(\tau) = \pi/2 + 2\tan^{-1}[\tanh[\sqrt{2V_0\rho_0/M}\tau]]. \tag{D11}$$

For $V_0 \gg 0$, $\partial_\tau\tilde{\phi}(\tau) \simeq \delta(\tau)$, where $\delta(\tau)$ is the delta function. The general solution of the field $\phi_0(\tau)$ is given by the linear combination of $\tilde{\phi}(\tau)$,

$$\phi_0(\tau) = \sum_i \epsilon_i\tilde{\phi}(\tau-\tau_i), \tag{D12}$$

where $\epsilon_i = \pm 1$, and $\sum_i\epsilon_i = 0$. By using (D12) and (D9), the partition function of the system is given by [5].

$$Z = \sum_{p=0}^{\infty}\Delta_0^{2p}\sum_{\epsilon_1=\pm1\ldots\epsilon_{2p}=\pm1}\int_0^\infty d\tau_{2p}\int_0^{\tau_{2p}}d\tau_{2p-1}\ldots\int_0^{\tau_2}d\tau_1 e^{2/K\sum_{i>j}\epsilon_i\epsilon_j\log(|\tau_i-\tau_j|/\delta)}, \tag{D13}$$

where $\Delta_0 = e^{-4\sqrt{2\rho_0V_0M}}$ and δ is the short time cutoff. Since, in the strong coupling limit $V_0 \gg 1$, the large number of instantons will give a small contribution to the partition function because of the pre-factor $\Delta_0 = e^{-4\sqrt{2\rho_0V_0M}}$, and the dominant contribution is given by one instanton and one anti-instanton.

For our calculation, we consider one instanton ($\epsilon_1 = 1$) and one anti-instanton ($\epsilon_2 = -1$). The field ϕ is given by

$$\phi_0(\tau) = \tilde{\phi}(\tau-\tau_1) - \tilde{\phi}(\tau-\tau_2), \tag{D14}$$

$$\begin{aligned}R_1(\tau) &= \langle\cos(2\phi_0(\tau))\cos(2\phi_0(0))\rangle\\ R_1(\tau) &= \left(1 + e^{-8\sqrt{2\rho_0V_0M}}\int_{-\beta/2}^{\beta/2}d\tau_1\int_{-\beta/2}^{\beta/2}d\tau_2\cos(2\tilde{\phi}(\tau-\tau_1) - 2\tilde{\phi}(\tau-\tau_2))\cos(2\tilde{\phi}(-\tau_1) - 2\tilde{\phi}(-\tau_2))(|\tau_1-\tau_2|/\delta)^{-2/K}\right)\\ &\times\left(1 + e^{-8\sqrt{2\rho_0V_0M}}\int_{-\beta/2}^{\beta/2}d\tau_1\int_{-\beta/2}^{\beta/2}d\tau_2(|\tau_1-\tau_2|/\delta)^{-2/K}\right)^{-1}\\ &\simeq -\frac{M^2}{2}e^{-8\sqrt{2\rho_0V_0M}}(|\tau|/\delta)^{-2/K}\end{aligned} \tag{D15}$$

where $\beta = 1/T$ and T is temperature. By using Appendix B, the imaginary part of $\langle\cos(2\phi_0(\tau))\cos(2\phi_0(0))\rangle(\omega)$ at $T = 0$ is given by

$$\mathrm{Im}[R_1(\tau)](\omega) = -M^2e^{-8\sqrt{2\rho_0V_0M}}\cos(\pi/K)\sin(\pi/K)\Gamma(1-2/K)(\delta\,\omega)^{2/K-1}. \tag{D16}$$

[1] I. Bloch, J. Dalibard, and W. Zwerger, Rev. Mod. Phys. **80**, 885 (2008).

[2] T. Esslinger, Annu. Rev. Condens. Matter Phys. **1**, 129 (2010).

[3] F. D. M. Haldane, J. Phys. C **14**, 2585 (1981).

[4] A. O. Gogolin, A. A. Nersesyan, and A. M. Tsvelik, *Bosonization and Strongly Correlated Systems* (Cambridge University Press, Cambridge, 2004).

[5] T. Giamarchi, *Quantum Physics in One Dimension (The International Series of Monographs on Physics)* (Clarendon Press, Oxford, 2004).

[6] M. A. Cazalilla, R. Citro, T. Giamarchi, E. Orignac, and M. Rigol, Rev. Mod. Phys. **83**, 1405 (2011).

[7] A. Georges and T. Giamarchi, arXiv:1308.2684.

[8] T. Giamarchi and H. J. Schulz, EPL (Europhys. Lett.) **3**, 1287 (1987).

[9] G. Roux, T. Barthel, I. P. McCulloch, C. Kollath, U. Schollwöck, and T. Giamarchi, Phys. Rev. A **78**, 023628 (2008).
[10] C. L. Kane and M. P. A. Fisher, Phys. Rev. B **46**, 15233 (1992).
[11] A. Furusaki and N. Nagaosa, Phys. Rev. B **47**, 4631 (1993).
[12] Z. Yao, H. W. C. Postma, L. Balents, and C. Dekker, Nature (London) **402**, 273 (1999).
[13] P. Fendley, A. W. W. Ludwig, and H. Saleur, Phys. Rev. Lett. **74**, 3005 (1995).
[14] A. Agarwal and D. Sen, Phys. Rev. B **76**, 035308 (2007).
[15] D. Makogon, V. Juricic, and C. M. Smith, Phys. Rev. B **74**, 165334 (2006).
[16] D. E. Feldman and Y. Gefen, Phys. Rev. B **67**, 115337 (2003).
[17] F. Dolcini, Phys. Rev. B **85**, 033306 (2012).
[18] T. Stöferle, H. Moritz, C. Schori, M. Köhl, and T. Esslinger, Phys. Rev. Lett. **92**, 130403 (2004).
[19] C. Schori, T. Stöferle, H. Moritz, M. Köhl, and T. Esslinger, Phys. Rev. Lett. **93**, 240402 (2004).
[20] C. D'Errico, E. Lucioni, L. Tanzi, L. Gori, G. Roux, I. P. McCulloch, T. Giamarchi, M. Inguscio, and G. Modugno, Phys. Rev. Lett. **113**, 095301 (2014).
[21] M. Endres, T. Fukuhara, D. Pekker, M. Cheneau, P. Schaubgr, C. Gross, E. Demler, S. Kuhr, and I. Bloch, Nature (London) **487**, 454 (2012).
[22] A. Iucci, M. A. Cazalilla, A. F. Ho, and T. Giamarchi, Phys. Rev. A **73**, 041608 (2006).
[23] A. Tokuno and T. Giamarchi, Phys. Rev. Lett. **106**, 205301 (2011).
[24] C. Kollath, A. Iucci, I. P. McCulloch, and T. Giamarchi, Phys. Rev. A **74**, 041604 (2006).
[25] A. Tokuno, E. Demler, and T. Giamarchi, Phys. Rev. A **85**, 053601 (2012).
[26] L. W. Cheuk, M. A. Nichols, M. Okan, T. Gersdorf, V. V. Ramasesh, W. S. Bakr, T. Lompe, and M. W. Zwierlein, Phys. Rev. Lett. **114**, 193001 (2015).
[27] E. Haller, J. Hudson, A. Kelly, D. A. Cotta, B. Peaudecerf, G. D. Bruce, and S. Kuhr, Nat. Phys. **11**, 738 (2015).
[28] D. Greif, L. Tarruell, T. Uehlinger, R. Jördens, and T. Esslinger, Phys. Rev. Lett. **106**, 145302 (2011).
[29] J. Catani, G. Lamporesi, D. Naik, M. Gring, M. Inguscio, F. Minardi, A. Kantian, and T. Giamarchi, Phys. Rev. A **85**, 023623 (2012).
[30] J. F. Sherson, C. Weitenberg, M. Endres, M. Cheneau, I. Bloch, and S. Kuhr, Nature (London) **467**, 68 (2010).
[31] M. Boll, T. A. Hilker, G. Salomon, A. Omran, J. Nespolo, L. Pollet, I. Bloch, and C. Gross, Science **353**, 1257 (2016).